the FEBS Journal

Synthesis and structural characterization of a mimetic membrane-anchored prion protein

Matthew R. Hicks[1], Andrew C. Gill[2], Imanpreet K. Bath[1], Atvinder K. Rullay[3], Ian D. Sylvester[2], David H. Crout[3] and Teresa J. T. Pinheiro[1]

1 Department of Biological Sciences, University of Warwick, Coventry, UK
2 Institute for Animal Health, Compton, Newbury, UK
3 Department of Chemistry, University of Warwick, Coventry, UK

Keywords
prion; GPI; membranes; conversion; rafts

Correspondence
T.J.T. Pinheiro, Department of Biological Sciences, University of Warwick, Gibbet Hill Road, Coventry, CV4 7AL, UK
Fax: +44 2476 523701
Tel: +44 2476 528364
E-mail: t.pinheiro@warwick.ac.uk

(Received 21 December 2005, revised 19 January 2006, accepted 23 January 2006)

doi:10.1111/j.1742-4658.2006.05152.x

During pathogenesis of transmissible spongiform encephalopathies (TSEs) an abnormal form (PrP^{Sc}) of the host encoded prion protein (PrP^{C}) accumulates in insoluble fibrils and plaques. The two forms of PrP appear to have identical covalent structures, but differ in secondary and tertiary structure. Both PrP^{C} and PrP^{Sc} have glycosylphospatidylinositol (GPI) anchors through which the protein is tethered to cell membranes. Membrane attachment has been suggested to play a role in the conversion of PrP^{C} to PrP^{Sc}, but the majority of *in vitro* studies of the function, structure, folding and stability of PrP use recombinant protein lacking the GPI anchor. In order to study the effects of membranes on the structure of PrP, we synthesized a GPI anchor mimetic (GPIm), which we have covalently coupled to a genetically engineered cysteine residue at the C-terminus of recombinant PrP. The lipid anchor places the protein at the same distance from the membrane as does the naturally occurring GPI anchor. We demonstrate that PrP coupled to GPIm (PrP–GPIm) inserts into model lipid membranes and that structural information can be obtained from this membrane-anchored PrP. We show that the structure of PrP–GPIm reconstituted in phosphatidylcholine and raft membranes resembles that of PrP, without a GPI anchor, in solution. The results provide experimental evidence in support of previous suggestions that NMR structures of soluble, anchor-free forms of PrP represent the structure of cellular, membrane-anchored PrP. The availability of a lipid-anchored construct of PrP provides a unique model to investigate the effects of different lipid environments on the structure and conversion mechanisms of PrP.

Transmissible spongiform encephalopathies (TSEs) are a family of fatal, neurodegenerative diseases that includes scrapie of sheep, bovine spongiform encephalopathy of cattle, chronic wasting disease in cervids, and Creutzfeldt–Jakob disease in humans. These diseases are characterized by astrocytic gliosis, neuronal apoptosis and deposition of an abnormally folded isoform of the host encoded prion protein, PrP^{C} [1]. PrP^{C} is a small,

Abbreviations
ATR, attenuated total reflection; DPPC, dipalmitoyl phosphatidylcholine; ER, endoplasmic reticulum; GPI, glycosylphospatidylinositol; GPIm, GPI anchor mimetic; LB, Luria–Bertani medium; MES, 2-(N-morpholino) ethanesulfonic acid; MOPS, 3-(N-morpholino) propanesulfonic acid; OG, octyl-β-D-glucopyranoside; POPC, 1-palmitoyl-2-oleoyl-phosphatidylcholine; PrP, prion protein; PrP-Glut, PrP–S231C with a disulfide bond between Cys179 and Cys214 and with a glutathione group disulfide-bonded to Cys231; PrP–GPIm, PrP–S231C with a disulfide bond between Cys179 and Cys214 and with a GPI mimetic disulfide bonded to Cys231; PrP-React, PrP–S231C with a disulfide bond between Cys179 and Cys214 and with Cys231 reduced; PrP–S231C, recombinant Syrian hamster prion protein, residues 23–231 (preceded by a methionine start codon) with Ser231 mutated to Cys; TSE, transmissible spongiform encephalopathy.

cell-surface glycoprotein, which is soluble in detergents and is protease sensitive [2]. In contrast, the abnormal form, PrP^{Sc}, is insoluble in most detergents and partially protease resistant, leading to accumulation of the protein in amyloid plaques and fibrils during disease. PrP^{Sc} is also believed to constitute the majority, if not all of the infectious agent in TSE diseases [3,4].

PrP^{C} is translated as a polypeptide of around 250 amino acids (depending on species) and contains two signal peptides, which are cleaved during post-translational processing [5]. An N-terminal signal peptide directs the protein to the endoplasmic reticulum (ER) for export, via the secretory pathway, to the outer leaflet of the plasma membrane, where it is anchored through a glycosylphospatidylinositol (GPI) anchor. Attachment of the GPI anchor to the C-terminus of PrP occurs in the ER by a transamidation reaction, following proteolytic cleavage of the C-terminal signal peptide. During post-translational processing in the secretory pathway, PrP^{C} can also be N-glycosylated with diverse oligosaccharides at two asparagine residues, towards the C-terminal end [6], and a single disulfide bond is formed, also towards the C-terminus [1].

Initial studies of the structure of PrP^{C} and PrP^{Sc} were carried out using FTIR spectroscopy and indicated that PrP^{C} is composed of $\sim$35% α helix and a small amount of β sheet, whereas PrP^{Sc} appears to have elevated levels of β sheet [7,8]. Higher resolution studies of the structure of PrP^{C} have made use of NMR and X-ray crystallography methods, but have focused almost entirely on analysis of recombinant forms of the protein that lack the lipid anchor and glycosylation. These studies show that PrP has a folded C-terminal domain, comprising approximately half of the protein's amino acid sequence [9,10]. This folded domain contains predominantly α-helical structure with a small amount of β sheet, in line with the early FTIR studies of PrP^{C}. The N-terminal half of the protein appears to be flexible and disordered and contains four octapeptide-repeat regions, which have been shown to bind copper ions [11–14]. The structure of recombinant PrP is assumed to represent the cellular form of PrP. A recent report on the structure of PrP^{C} purified from healthy calf brains further supports this assumption [15]. In this study the protein is natively folded and retains the two glycosyl moieties but is cleaved from the GPI anchor and therefore released from the membrane surface.

There is no high-resolution structure of PrP^{Sc}, but models have been constructed based initially on the accessibility of antibody-binding epitopes and, more recently, on electron crystallography measurements. The best current models suggest that PrP^{Sc} adopts parallel β sheet structures with the PrP sequence from residues 89–175 forming a trimeric α-helical conformation, whereas the C-terminal region (residues 176–227) retains the disulfide-linked, α-helical conformation present in PrP^{C} [16,17].

The normal cell biology of PrP^{C} involves rapid, constitutive endocytosis from the plasma membrane [18], an event that requires interaction with additional cell-surface molecules. Like other GPI-anchored proteins, PrP^{C} occupies specialized domains on the cell surface known as lipid rafts [19], but appears to move out of rafts prior to endocytosis [20]. Conversion from PrP^{C} to PrP^{Sc} is thought to take place either on the cell surface [21–23], perhaps in lipid rafts [19,24–28], or during internal transit in the endocytic pathway [27,29–31]. It is also thought that partial unfolding is necessary, potentially assisted by accessory molecules. If conversion is indeed a cell-surface event, this requires a thorough understanding of the folding and interactions of PrP in its tethered conformation on the plasma membrane.

The interaction of PrP with different lipid components is complex and is not completely understood. Previously, we have shown that anchorless forms of PrP bind to lipid membranes [32–34]. This interaction involves both an electrostatic and a hydrophobic component. The composition of the membranes and conformation of PrP affect the strength of the binding and the propensity for aggregation of the protein. It was found that membranes can be disrupted by PrP under certain conditions [33,34]. Also, whereas some membranes lead to extensive aggregation or fibrillization of PrP, others appear to provide protection against conversion [34,35].

To date, most structural studies have been carried out on protein that does not contain a lipid anchor. However, as outlined above, there is considerable evidence that membrane-anchored forms of PrP are involved in the pathological conversion process. In order to study the structure of PrP in a context closer to that found *in vivo*, we synthesized a GPI-mimetic (GPIm) that can be coupled to the C-terminus of PrP by reaction with the free thiol group of a genetically engineered cysteine residue. This lipid-modified PrP molecule (PrP–GPIm) was reconstituted into different model membranes. The structure of PrP–GPIm inserted in lipid membranes was studied using infrared spectroscopy. The lipid composition of the membrane was chosen to represent the cellular environments in which the protein is found *in vivo*, such as inside or outside lipid rafts, and studies were carried out at neutral and acidic pH values to represent the pH at

the plasma membrane and in endocytic vesicles, respectively.

Results

A previous report by Eberl *et al.* [36] detailed the characterization of recombinant PrP inserted in lipid membranes. This protein has a hydrophilic C-terminal extension of five glycines and a cysteine residue, which was coupled to a thiol-reactive lipid, *N*-((2-pyridyldithio)-propinyl)-1,2-dihexadecanoyl-*sn*-glycero-3-phosphoethanolamine. We used a similar principle to covalently attach a synthetic lipid to the thiol group of an engineered cysteine at the C-terminus of PrP, taking a somewhat different strategy. A cysteine residue replaces Ser231, in which the natural GPI anchor is coupled to PrP, and we used a synthetic lipid anchor which carries a linker region based on ethylene-glycol units (Experimental procedures). This linker places the protein at a distance from the membrane surface similar to that provided by the glycan moiety in the reported natural GPI anchor [37]. Several steps are required to couple the lipid anchor to PrP–S231C. During these steps, it is essential to maintain a free thiol at the C-terminal cysteine, while retaining an intact internal disulfide bond in PrP.

Expression, purification and refolding of PrP–S231C

The C-terminal serine residue of Syrian hamster PrP was altered genetically to a cysteine residue by site-directed mutagenesis to produce the construct SHaPrP–S231C. The protein was expressed as insoluble inclusion bodies in *Escherichia coli* and purified by size-exclusion chromatography followed by reversed-phase HPLC (see Experimental procedures). After lyophilization, the protein was resuspended in an oxidation buffer containing both oxidized and reduced glutathione, using a method modified from Mo *et al.* [38]. This reaction produced primarily monomeric PrP containing a single, native, internal disulfide bond with the C-terminal Cys231 protected by a glutathione molecule (PrP-Glut). This was confirmed by on line HPLC- MS analysis (Fig. 1A).

The equivalent PrP Cys mutant, $PrP(Gly)_6Cys$, of Eberl *et al.* [36] was refolded by disulfide oxidation on Ni-NTA columns, followed by selective reduction of disulfides in the resulting dimeric species. We attempted the method described in Eberl *et al.* but found that glutathione-mediated reoxidation formed the correct product more specifically and in significantly higher yields. The glutathione protecting group was removed by brief treatment with dithiothreitol; the resulting product was purified by HPLC (Fig. 1B) and was found by HPLC-MS analysis to have an intact internal disulfide bond and a reduced C-terminal cysteine

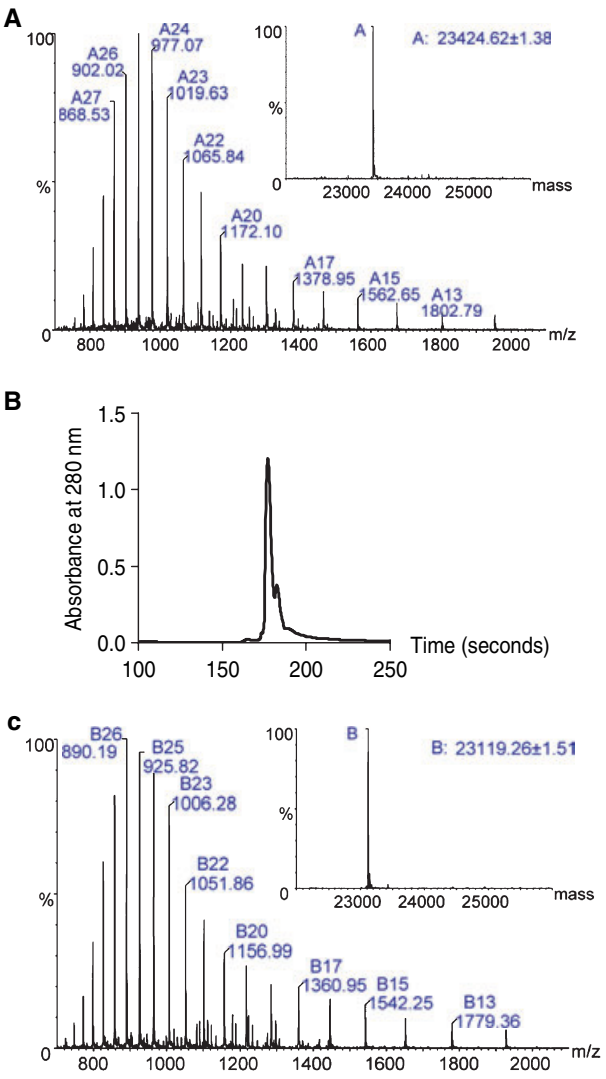

Fig. 1. MS characterization and HPLC separation of refolded states of PrP–S231C. (A) Electrospray MS and deconvoluted MS (inset) of PrP-Glut after refolding of PrP–S231C in the presence of glutathione. The measured mass (23 424.6 Da) is in good agreement with the calculated mass (23 423.9 Da) for PrP with an intact internal disulfide bond and a modified C-terminal Cys231 residue with a single glutathione molecule. (B) HPLC purification of PrP-Glut after treatment with the reducing agent dithiothreitol to give PrP-React. The main peak is the desired product and the smaller shoulder is fully reduced material that was discarded by peak cutting. (C) Electrospray MS and (inset) deconvoluted MS of PrP-React. The measured mass (23 119.3 Da) agrees with the calculated mass (23 118.6 Da) for PrP with an internal disulfide bond and the presence of a free thiol group on Cys231.

(Cys231) (Fig. 1C). This process created a reasonable yield of the correctly folded PrP molecule with a free thiol at Cys231, which we refer to as PrP-React.

Coupling of PrP-React to GPIm

We synthesized a mimetic of a GPI membrane anchor, GPIm, according to the reaction scheme described in Experimental procedures. The chemical structure of GPIm is shown in Fig. 2A. Coupling of GPIm to the engineered C-terminal cysteine residue in PrP–S231C occurs via a nucleophilic attack by the thiolate anion of the cysteine side chain on the methane thiosulfonate group of GPIm, producing a disulfide linkage between PrP and the lipid tail. The resulting lipid-modified protein enables incorporation of PrP into lipid membranes (Fig. 2B).

In trial coupling reactions, we determined that the efficiency of the coupling reaction is dependent on several factors. These include the solubility of both GPIm and PrP-React, temperature, pH, the reaction time and the ionic strength of the solution. Optimum solubility of lipids, such as GPIm, is typically achieved by the use of organic solvents. Several solvents were investigated, including ethanol, methanol and dimethylsulfoxide, giving similar results. The solubility of GPIm at different ethanol concentrations is shown in Fig. 3A. Concentrations above 60% (v/v) ethanol in water were required to maintain GPIm in solution, and, consequently, allowed the coupling reaction to proceed at acceptable yields (Fig. 3B). The reaction should also proceed more rapidly at a higher pH, under which conditions the proportion of cysteine that is in the reactive, anionic form will be increased. However, we found that increasing the pH of the reaction buffer resulted in a decrease in the yield, probably due to decreased solubility of PrP-React in water/ethanol at high pH. It is also possible that the two positively charged arginine residues adjacent to Cys231 in the primary structure of PrP may lower the effective pK_a of the cysteine side chain by stabilizing the negatively charged thiolate anion, thereby helping the reaction to proceed at lower pH. Our final empirically determined reaction protocol involves the use of 70% (v/v) ethanol in water, 10-fold molar excess of GPIm and incubation at room temperature for 2 h. The use of buffer (MES or MOPS) even at low concentrations (2 mM) resulted in a decrease in the yield (data not shown). This was probably due to a decrease in the solubility of the protein in ethanolic solutions in the presence of salts. For this reason, buffers were not added to the coupling reactions. The apparent pH of the ethanolic

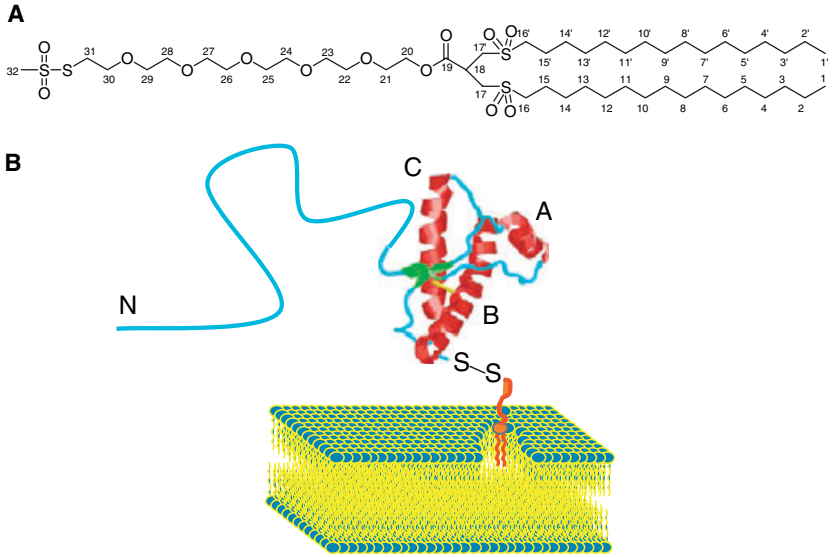

Fig. 2. Membrane-anchored PrP–GPIm. (A) Chemical structure of the mimetic GPI anchor (GPIm): 3-(Hexadecane-1-sulfonyl)-2-(hexadecane-1-sulfonylmethyl) propionic acid 2-[2-(2-[2-[2-(2-methanesulfonylsulfanylethoxy)ethoxy]ethoxy}ethoxy)ethoxy] ethyl ester, synthesized according to the reaction scheme described in Experimental procedures. (B) Schematic diagram of PrP–GPIm anchored in a lipid membrane. GPIm is shown in orange coupled to the C-terminal Cys residue (Cys231) at the end of helix C via a disulfide bond (S–S). The lipid membrane is represented by a fragment of a bilayer formed by ideally packed lipid molecules, comprising a hydrophilic head group (dark blue circles) and hydrophobic acyl chains (yellow tails). The folded C-terminal domain of the protein shows the three helices in red (A, B, C) and the small antiparallel β sheet in green [41]. The N-terminal portion (residues 23–126) has no defined high-resolution structure and is shown schematically in light blue with N labelling the N-terminus. The internal disulfide bond between the two main helices (B and C) is shown in yellow.

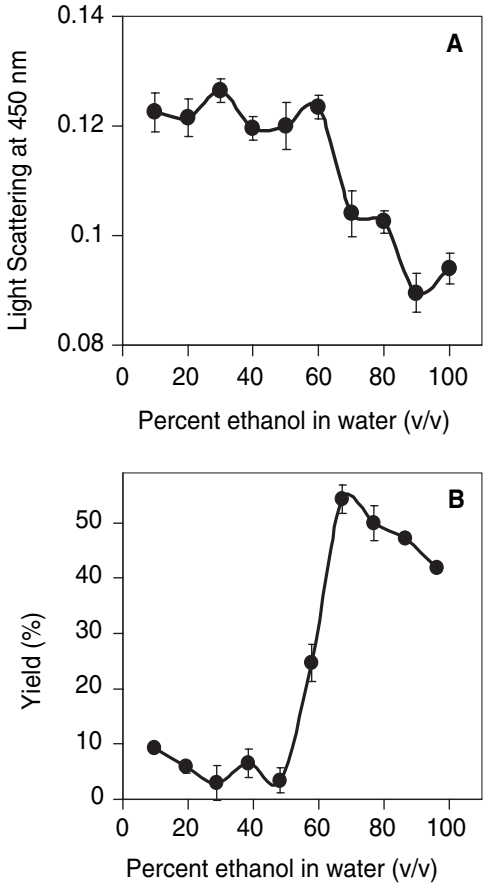

Fig. 3. Solubility and reactivity of the lipid anchor GPIm in ethanol/water mixtures. (A) The solubility in ethanol/water mixtures was monitored by light scattering at 450 nm. Insoluble GPIm creates a suspension that scatters light and gives a large signal. As the ethanol concentration increases the GPIm stays in solution and therefore scatters less light and gives a smaller signal. (B) The efficiency of the coupling reaction between PrP-React and GPIm was monitored by peak area of the product on an HPLC gradient. Maximal product was obtained around 70% ethanol.

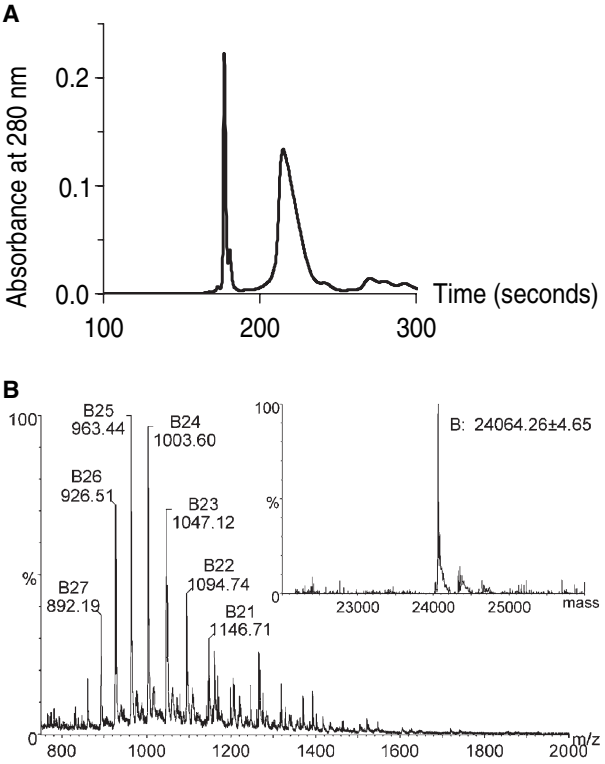

Fig. 4. HPLC purification and MS characterization of PrP–GPIm. (A) After reaction of PrP-React with GPIm, the product PrP–GPIm was purified by RP-HPLC. The product elutes as a broad peak at around 220 s and uncoupled material elutes at around 180 s. (B) Electrospray MS and deconvoluted MS (inset) of PrP–GPIm. The measured mass of 24 064.3 Da agrees with the expected calculated mass of 24 064.1 Da for PrP with one coupled GPIm molecule and an intact internal disulfide bond.

solutions was measured and found to be ~pH 6. Typically, 0.5 mg of PrP–GPIm were obtained per mg of PrP-React. Correctly formed product, PrP–GPIm, was separated from noncoupled PrP-React by RP-HPLC (Fig. 4A) and the molecular mass of the product was confirmed by HPLC-MS (Fig. 4B).

Reconstitution of PrP–GPIm into membranes

PrP–GPIm was anchored in lipid membranes through the insertion of the hydrocarbon chains of GPIm into the lipid bilayer. Several methods are commonly used to reconstitute integral membrane proteins and GPI-anchored proteins into membranes [39,40]. Our approach was to preform liposomes, partially disrupt them with detergent and mix with PrP–GPIm. Upon detergent removal, liposomes are reformed, in which PrP–GPIm is anchored.

The concentration of the detergent octyl-β-D-glucopyranoside (OG) required to induce a phase break in the liposomes was determined by titration of a concentrated stock of OG into a suspension of liposomes [39]. The turbidity was monitored at 350 nm and solubility curves identified for both 1-palmitoyl-2-oleoylphosphatidylcholine (POPC) and raft liposomes (Fig. 5). The concentration of OG at the midpoint of the transition was found to be 22 mM for POPC and 28 mM for rafts at 20 °C.

After detergent dialysis, reconstituted liposomes containing PrP–GPIm were separated on sucrose gradients and analysed by SDS/PAGE (see Experimental procedures). Eight fractions spanning the entire sucrose gradient were collected and the lipid was visible as a

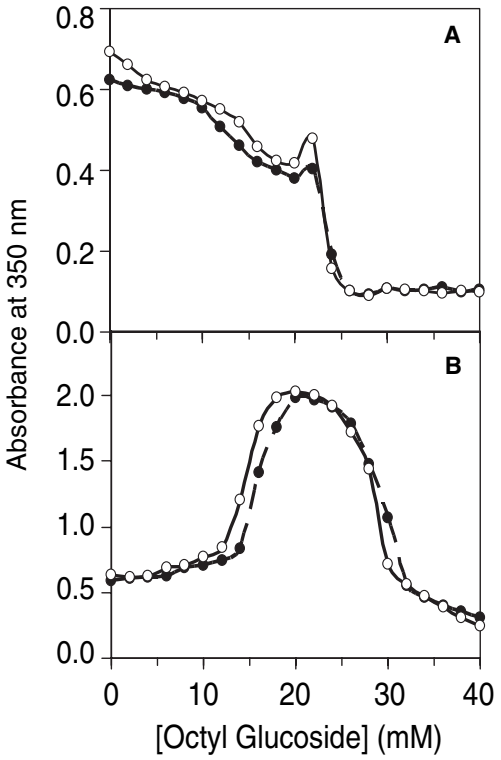

Fig. 5. Solubilization of liposomes by the detergent OG at 20 °C. Liposomes formed by extrusion at pH 7 (○) and at pH 5 (●) were titrated with OG and the turbidity was monitored at 350 nm. The drop in turbidity above 20 mM OG represents the detergent-solubilization of liposomes. (A) POPC liposomes at pH 7 (○) and pH 5 (●). (B) Raft liposomes at pH 7 (○) and at pH 5 (●).

turbid band in the top three fractions for POPC samples and mainly in fraction 3 for raft samples. The majority of PrP–GPIm co-migrated with the liposomes (Fig. 6). The fraction of PrP–GPIm that was associated with the liposomes was assessed by densitometry of the bands on the SDS/PAGE gels in the first three lanes as a percentage of the total across all eight sample lanes. Reconstitution efficiencies appeared independent of pH and were ~90% for POPC liposomes and ~70% for raft liposomes.

Structure of PrP–GPIm in liposomes

The structure of PrP–GPIm was compared with that of anchorless recombinant PrP(23–231), which also lacks the glycosylation, and for convenience is here referred as wild-type PrP (PrP-WT). The structures of PrP–GPIm and PrP-WT in solution were probed by CD and attenuated total reflection (ATR) FTIR. The far-UV CD spectrum of PrP-WT shows the typical minima around 208 and 222 nm (Fig. 7A) associated with proteins containing predominantly α-helical structure. In contrast, the CD spectrum of PrP–GPIm shows a single broad minimum around 214 nm and a characteristic loss in signal intensity, which are typical for a β-sheet structure. These spectral properties indicate that PrP–GPIm in solution has an elevated content of β sheet relative to PrP-WT. These results are consistent with the spectral changes observed using ATR FTIR. The amide I region of the FTIR spectrum

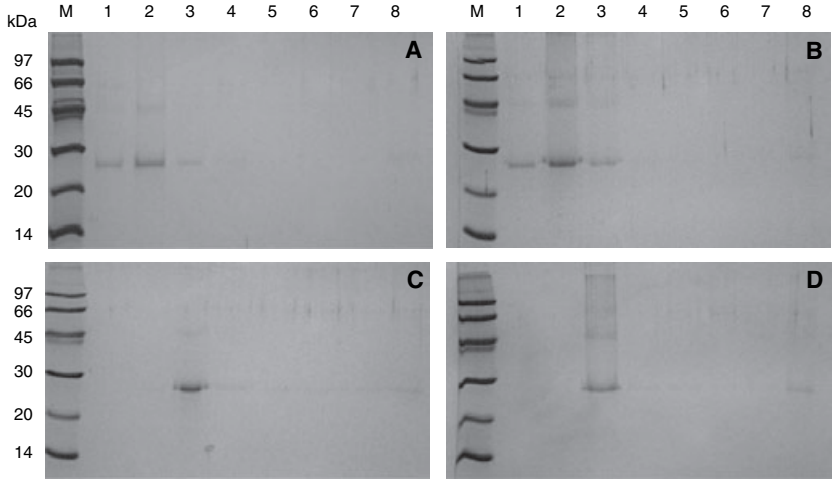

Fig. 6. SDS/PAGE of fractions from density gradient separation of reconstitutions of PrP–GPIm in lipid membranes. Membrane reconstitutions of PrP–GPIm were separated on sucrose step gradients and eight fractions spanning the entire sucrose gradient were collected from top-to-bottom. The fractions were analysed for protein by SDS/PAGE. From left to right the lanes are markers (M) and the eight fractions (labelled 1–8) from the gradient. Samples of PrP–GPIm were reconstituted into vesicles containing (A) POPC at pH 5, (B) POPC at pH 7, (C) rafts at pH 5 and (D) rafts at pH 7. Lipid was visible in fractions 1–3 for POPC (A, B) and in fraction 3 for raft lipids (C, D). The majority of the protein co-migrated with the liposomes in the sucrose gradient.

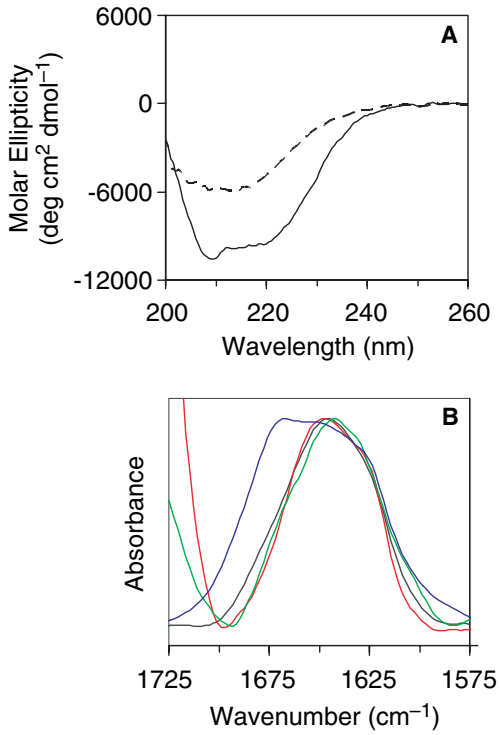

Fig. 7. Structure of PrP–GPIm compared with PrP-WT in solution. (A) Far-UV CD spectra of PrP-WT (solid line) and PrP–GPIm (dashed line) in solution at pH 5. (B) The amide I region of ATR FTIR spectra of PrP-WT (black) and PrP–GPIm (blue) in solution at pH 5 compared with PrP–GPIm after reconstitution into POPC (red) and raft membranes (green) at pH 5.

for PrP–GPIm and PrP-WT is shown in Fig. 7B. The amide I band arises mainly from stretching modes of the backbone carbonyl bonds in the protein. The positions of absorbance bands are dependent on secondary structure and therefore can be used to measure the amount of different types of secondary structure in proteins. Because the bands overlap it is necessary to use peak-fitting analysis to deconvolute the contributions from different secondary structural components. The amide I band of PrP-WT in solution is centered around 1645 cm^{-1} due to the contribution from both random coil (30%) and α-helical structure (32%). There are also contributions from β sheet (21%) and β turns (17%). Although the levels of β sheet measured here are greater than the level predicted from NMR structures of the folded C-terminal domain of PrP (residues 90–231) [41], the differences may be attributable to the adoption of a β-sheet-like extended structure by the N-terminal region of PrP comprising residues 23–90 upon deposition on the ATR crystal. Although the N-terminal region is traditionally thought of as flexible and unstructured, several recent papers have indicated that stable, extended structures are present within this domain [42–44]. The ATR FTIR spectrum of PrP–GPIm in solution is distinct from that of PrP-WT (Fig. 7B). Secondary structure calculations suggest that PrP–GPIm in solution has a higher content of β sheet compared with the anchorless protein (PrP–GPIm has 37% β sheet compared with 21% in PrP-WT) at the expense of α helix (32% in PrP-WT, 19% in PrP–GPIm) and some random coil (30% in PrP-WT, 23% in PrP–GPIm).

After insertion of PrP–GPIm into membranes, ATR FTIR spectra were acquired for POPC and raft membranes containing PrP–GPIm at pH 5 and 7. The amide I region of the ATR FTIR spectrum for PrP–GPIm inserted in POPC and raft membranes, at pH 5, is shown in Fig. 7B. Insertion of PrP–GPIm into lipid membranes returns the structure of PrP to the original α-helical structure of PrP-WT. Similar spectra were observed for reconstituted PrP–GPIm at pH 7 (data not shown). The secondary structure content, estimated from peak-fitting analysis, was found to be very similar to that of PrP-WT. These results indicate that PrP–GPIm in POPC and raft membranes have a very similar structure and demonstrate that the structure of PrP in these membranes resembles the structure of anchorless protein in solution.

Discussion

Membrane-anchored PrP has a similar structure to soluble anchorless PrP

There are several published methods by which lipid anchored proteins can be reconstituted into liposomes. Reconstitution of proteins into membranes for subsequent structural or functional studies requires that the method used does not perturb the native structure of the protein irreversibly. Most methods involve the use of detergent, which can often adversely affect protein structure [39]. The best method for the reconstitution of a particular protein often has to be determined empirically.

We attempted various methods for reconstituting PrP–GPIm into membranes. Spontaneous insertion of the lipid-anchored protein into preformed liposomes did not occur; this may be due to a low partition energy between PrP–GPIm in solution and PrP–GPIm anchored in the membrane. Two observations are consistent with this interpretation: first, the lipid-modified protein (PrP–GPIm) was readily soluble in water and second, the structure of PrP–GPIm in solution was altered relative to the anchorless protein (PrP-WT) (Fig. 7). The latter suggests an interaction of the lipid

anchor with the protein in the absence of membranes, which may explain why spontaneous membrane insertion of PrP–GPIm was not observed. However, the use of OG promoted the insertion of PrP–GPIm into liposomes, producing a membrane-reconstituted protein in which the normal α-helical structure of PrP is restored (Fig. 7B).

Solution NMR structures of various recombinant forms of prion proteins, all lacking a GPI anchor, have been proposed to represent the structure of the cellular form of PrP anchored in the cell membrane [41,45,46]. Furthermore, molecular dynamic calculations revealed that the glycan region in the natural GPI of PrP was highly flexible [47], which led to the speculation that PrP could adopt a wide range of orientations relative to the plane of the cell membrane. Some of these orientations would allow the possibility of direct interactions of the protein with the membrane surface, which could lead to a different protein structure relative to the reported structures of anchorless PrP in solution. To test these possibilities, membrane reconstitution of a lipid-anchored form of PrP is imperative.

Reconstitution of PrP–GPIm in two types of model membranes, POPC and raft membranes, at either pH 7 or 5, resulted in a conformation of PrP that resembles the anchorless protein in solution. Similar findings were reported by Eberl *et al.* [36] with an alternate membrane-anchored PrP construct. In both Eberl *et al.*'s and the present lipid-modified PrP constructs, the prion protein is placed at a distance from the membrane surface via a linker region which mimics that provided by the flexible glycan moiety of the natural GPI anchor in PrP. In the PrP construct of Eberl *et al.* this linker is made of five Gly residues at the C-terminus of the protein, whereas in our protein the linker is provided by six ethylene-glycol units in the hydrophilic portion of the lipid molecule (Fig. 2A). The independent results from both laboratories using different constructs of GPI-anchored PrP, show unequivocally that GPI-anchored prion protein, when reconstituted in POPC and raft membranes, retains the structural characteristics of PrP-WT in solution. Therefore, the results strongly suggest that when PrP is localized in phosphatidylcholine-rich lipid environments in the plasma membrane of neurons or within rafts *in vivo*, the protein has a similar structure to that of the soluble anchorless forms determined by NMR spectroscopy.

Prion conversion and membranes

Cell biology studies implicate the plasma membrane surface as the likely site of prion conversion [19,48,49]. Because the prion protein is predominantly localized within cholesterol- and sphingomyelin-rich domains, or lipid rafts, in its cell-anchored form, it has been proposed that PrP conversion is likely to occur in rafts. Several lines of evidence implicate lipid rafts in prion conversion, but their precise role in this process is not fully understood and contradictory reports exist [50]. Some cell biology experiments appear to indicate that conversion could occur inside rafts, whereas others support conversion outside rafts. The precise lipid environment experienced by PrP may be a crucial factor in prion pathogenesis. Recent studies have shown that the prion protein moves out of rafts before being endocytosed and rapidly recycled back to the cell surface [51]. This movement of PrP in and out of rafts exposes PrP to different lipid environments, which may affect the structure of PrP. Furthermore, prion plaques and aggregates extracted from diseased brains have been shown to contain lipids [52], which further supports the hypothesis that conversion must occur at the membrane surface and lipid may be involved in the actual molecular mechanism of prion conversion.

A lipid-mediated conversion process of PrP is particularly relevant in sporadic cases of TSEs in which, by an as a yet unknown mechanism, the normal cellular form of PrP is spontaneously converted to aberrant aggregated forms associated with disease. An anomalous interaction of PrP with lipid could provide the initial unknown factor in spontaneous formation and subsequent accumulation of abnormal conformations of PrP. Therefore, *in vitro* studies employing a lipid-anchored prion molecule offer the potential to unravel the effect of different lipid environments on prion structure and conversion.

Previous studies have shown that anchorless forms of PrP can interact with various model lipid membranes and that this results in protein structural changes that lead to aggregation and/or fibrillization of PrP, depending on the lipid environment and starting conformation of the protein [33,34]. The α-helical isoform of PrP, representing the cellular prion protein, can bind to raft membranes but this does not induce aggregation of PrP. In contrast, an altered β-sheet-rich form of PrP has a high affinity to raft membranes resulting in prion fibrillization. Binding of α-helical and β-sheet-rich forms of PrP to negatively charged lipids, typically found outside rafts in cell membranes, results in amorphous aggregation of prion proteins. These results, combined with the observed rapid transit of PrP in and out of rafts [51], have led us to propose that early steps in the conversion of PrP from its cellular, α-helical conformation to altered β-sheet-rich states, prone to aggregation, may occur outside rafts [50]. Upon re-entry in rafts, β-sheet-rich forms of PrP

have higher affinities to raft lipid components and aberrant prion molecules may start to accumulate within rafts, promoting protein–protein interactions, which ultimately result in aggregation and fibrillization of PrP.

We have previously investigated the interaction of soluble, anchorless α-helical PrP with raft and POPC membranes. The truncated protein, PrP(90–231), was found to bind to rafts at pH 7 and not at pH 5 [34]. This interaction results in an increase in α-helical structure and no detectable protein aggregation. More importantly, the full-length protein, PrP(23–231), does not bind to rafts or POPC vesicles either at pH 7 or 5 (Correia B. *et al.*, University of Warwick, unpublished results). Therefore, in POPC and raft membranes, anchorless forms of prion proteins either do not interact with these lipids (full-length construct) or if they do (truncated form), no detrimental structural changes that would lead to aggregation are observed. In the current study, insertion of lipid anchored construct PrP–GPIm into POPC and raft membranes results in protein that regains its α-helical structure, producing FTIR spectra that are similar to those of soluble constructs of anchorless PrP. The results suggest that the lipid raft environment protects the α-helical conformation of PrP, in line with our hypotheses that conversion is initiated outside rafts [50].

Experimental procedures

Expression and purification of PrP

The plasmid (pTrcSHaPrPMet23–231) encoding the Syrian hamster prion protein was prepared as described previously [53]. The mutant protein PrP–S231C was constructed by site directed mutagenesis of pTrcSHaPrPMet23–231 using a QuikChange® kit (Stratagene, Amsterdam Zuidoost, the Netherlands) according to the manufacturer's instructions. Briefly, the complimentary mutagenic primers (IDS12A, 5′-CGATGGAAGAAGGTGCTGAGAATTCGAAGC-3′ and IDS12B, 5′-GCTTCGAATTCTCAGCACCTTCTTCCA TCG-3′) were synthesized and purified by MWG-Biotech AG (Ebersberg, Germany) to their 'high-purity salt free' standard. The mutagenesis reaction was performed in a thermal cycler using the following conditions: 1 cycle of (30 s at 95 °C) and 15 cycles of (30 s at 95 °C, 1 min at 55 °C and 10 min at 68 °C). Mutant clones were identified by DNA sequencing. The resulting plasmid will be referred to as pPrP–S231C.

pPrP–S231C was used to transform the protease-deficient strain of *E. coli*, BL21Star (Invitrogen, Paisley, UK). This strain had already been transformed with the Rosetta plasmid (Novagen, Darmstadt, Germany), which codes for mammalian tRNAs that are rare or absent in *E. coli*. Transformed cells were grown overnight at 37 °C on Luria–Bertani (LB) agar containing ampicillin (100 $\mu g \cdot mL^{-1}$) and chloramphenicol (37 $\mu g \cdot mL^{-1}$). A single colony was grown in LB medium until an absorbance of 0.6 at 600 nm was reached. Protein expression was then induced by the addition of 0.1 mM isopropyl-D-thiogalactopyranoside and the cells grown for a further 16 h. PrP–S231C is expressed in inclusion bodies. Cells were harvested by centrifugation and disrupted by sonication. Inclusion bodies were isolated by centrifugation at 27 000 ***g*** for 30 min and washed twice in 25 mM Tris/HCl pH 8.0, 5 mM EDTA. The inclusion bodies were solubilized in 8 M guanidine hydrochloride, 25 mM Tris/HCl pH 8.0, 100 mM dithiothreitol. The solubilized reduced PrP–S231C was applied to a size-exclusion column (Sephacryl S-300 H 26/60, Amersham Biosciences, Chalfont St. Giles, UK) and eluted in 6 M guanidine hydrochloride, 50 mM Tris/HCl pH 8.0, 5 mM dithiothreitol, 1 mM EDTA. Fractions containing reduced PrP–S231C were then applied to a reverse-phase HPLC column (Poros R1 20, Applied Biosystems, Foster City, CA) and eluted in a water/acetonitrile gradient in the presence of 0.1% (v/v) trifluoroacetic acid. The purified, reduced PrP–S231C was lyophilized. Yields of 15–25 mg of reduced PrP–S231C per litre of culture were typically obtained.

Oxidation of reduced PrP–S231C

Formation of the native disulfide bond was carried out, using a method modified from Mo *et al.* [38]. Briefly, reduced PrP–S231C at a concentration of 1 $mg \cdot mL^{-1}$ in 8 M guanidine hydrochloride, 25 mM Tris/HCl pH 8.0, was added drop-wise to 9 vol. of 50 mM Tris/HCl, 0.6 M L-arginine, 5 mM reduced glutathione, 0.5 mM oxidized glutathione pH 8.5 and left stirring overnight at 4 °C. The sample was centrifuged at 4500 ***g*** at 4 °C for 15 min to remove any precipitate and the supernatant was dialysed against 10 mM Tris/HCl pH 7.2. Precipitated protein (containing aggregated PrP) was removed using a 0.2 μm filter. The supernatant contained PrP with the native disulfide bond and glutathione-protected C-terminal cysteine (Cys231). The glutathione-protecting group on Cys231 was removed by treatment with 10 mM dithiothreitol for 10 min. The protein was applied to a reverse-phase HPLC column (Poros R1 20, Applied Biosystems) and eluted in a water/acetonitrile gradient in the presence of 0.1% (v/v) trifuoroacetic acid. The resulting purified PrP-React was lyophilized. The yield of the oxidation reaction followed by dialysis and subsequent removal of precipitated protein was typically 80% of the reduced protein obtained. This gave an overall yield of PrP-React of 12–20 mg per litre of culture.

Synthesis of the mimetic GPI anchor

In order to couple the synthetic lipid anchor to the protein, the reactive leaving group methanethiosulfonate (Scheme 1) was used. This was chosen because of the specific and quantitative reactivity of thiols towards it [54].

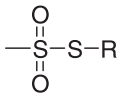

Scheme 1

Following the method of Ferris [55], the inexpensive and widely available diethyl bis(hydroxymethyl)malonate **1** and 48% HBr were heated under reflux at 140 °C with distillation of ethyl bromide, to afford 3-bromo-2-bromomethylpropanoic acid **2** as a crude pale brown solid, which was reduced according to the method of Ansari *et al.* [56] to 3-bromo-2-bromomethylpropan-1-ol **3** with diborane (B_2H_6) and tetrahydrofuran (THF) in dichloromethane (DCM) in an overall yield of 44% (Scheme 2).

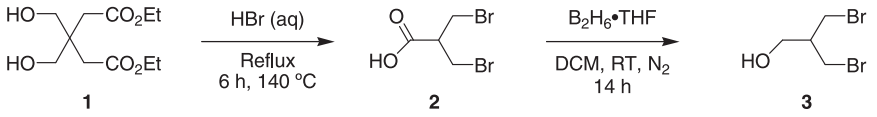

Scheme 2

It is noteworthy that formation of the α,β-unsaturated carboxylic acid (Scheme 3) was observed via elimination of HBr during synthesis of dibromoacid **2**. It was important to make sure the diacid **2** was pure before either reduction to alcohol or reaction with hexadecanethiol. Failure to do so made purification more difficult.

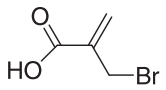

Scheme 3

Using the method employed by Zhang & Magnusson [57], dibromo alcohol **3**, hexadecanethiol **4** and caesium carbonate ($CsCO_3$) in dimethylformamide was stirred at room temperature for 24 h to give 3-hexadecylthio-2-(hexadecylthiomethyl) propan-1-ol **5** in good yield of 88% after crystallization from methanol (Scheme 4).

Although there are many methods available for the oxidation of alcohols, a reagent was required that would oxidize both the alcohol and the sulfide in a single step and in good yield. Potassium permanganate ($KMnO_4$) was chosen for the oxidation step, as was utilized by Georges *et al.* [58] for the oxidation of sulfides. A solution of potassium permanganate in water was added to a mixture of dithiolalkyl alcohol **5** in acetic acid at 60 °C and stirred for 24 h, resulting in the oxidized sulfone **6** (Scheme 4).

The first step in the synthesis of the spacer was the mono-*tert*-butyldimethylsilyl protection of hexaethylene glycol. Using the method of Bertozzi & Bednarski [59],

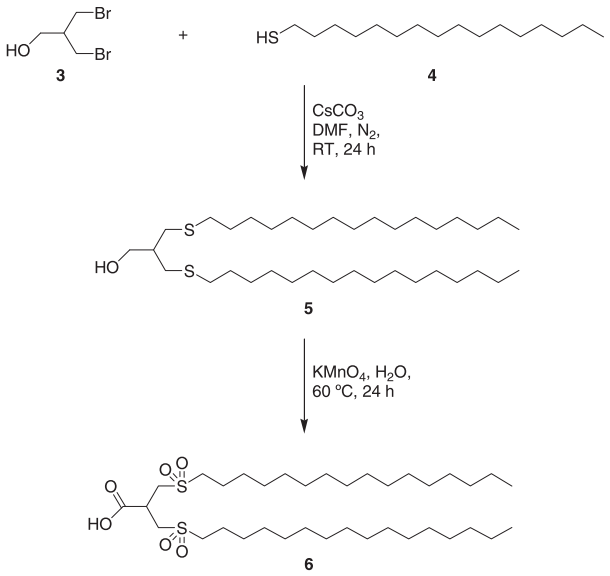

Scheme 4

reaction of hexaethyleneglycol with TBDMS-Cl (tert-butyldimethylsilyl chloride) and NaH (sodium hydride) at 0 °C gave a mixture of mono-substituted alcohol **7** and some di-substituted product which were easily separated by silica chromatography (Scheme 5).

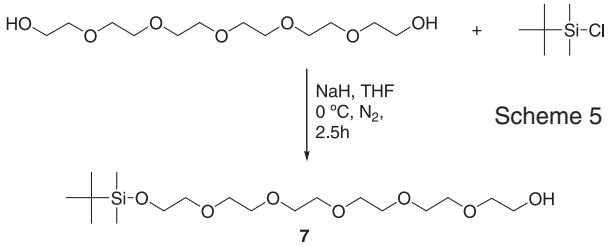

Scheme 5

Coupling of the sulfone-containing acid **6** with the mono-protected alcohol **7** was attempted using 1-ethyl-3-(3′-dimethylaminopropyl)carbodiimide (EDCI), a standard peptide coupling reagent. However, reactions using EDCI gave unsatisfactory yields of the required products. The alcohol was dried via Dean–Stark distillation to remove residual water that could not be removed by drying over P_2O_5 or in a vacuum oven. This improved the yield of product but was still unsatisfactory. However, using dicyclohexylcarbodiimide (DCC) and dimethylaminopyridine (DMAP) in DCM as utilized by Whitesell & Reynolds [60], provided a low but workable yield for coupling of the alcohol with the sulfone-containing acid to provide the ester **8** (Scheme 6).

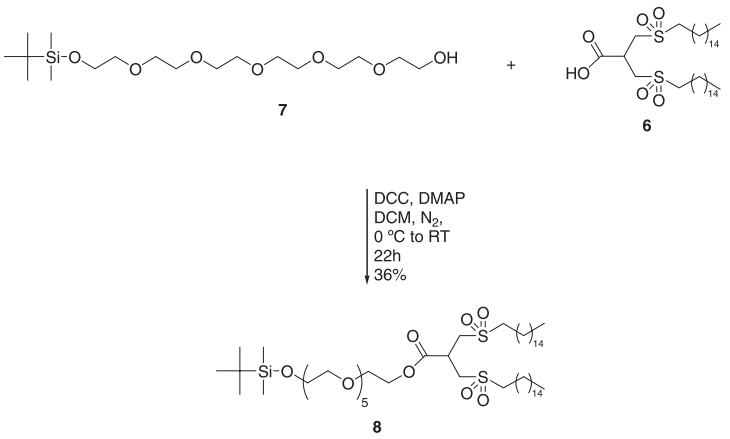

Scheme 6

TBDMS-protected lipid **8** was deprotected quantitatively using trifluoroborane etherate (BF_3OEt_2) in a mixture of dichloromethane and acetonitrile (CH_3CN) at 0 °C according to the procedure employed by King *et al.* [61]. The resulting alcohol **9** was reacted with methanesulfonyl chloride (CH_3SO_2Cl) in pyridine at 0 °C to give the mesylated derivative **10** in quantitative yield (Scheme 7).

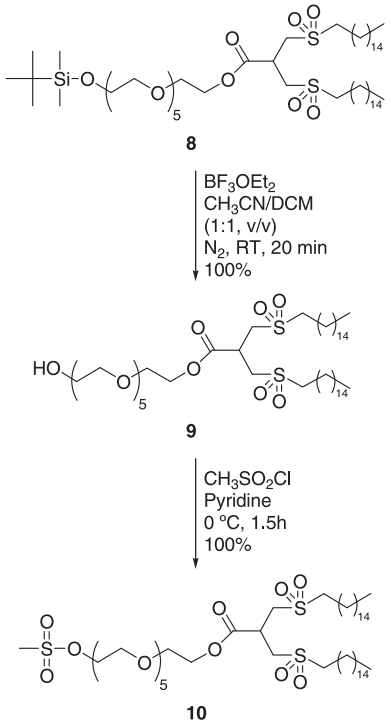

Scheme 7

The reaction of sodium methanethiosulfonate normally proceeds via displacement of bromine from a haloalkane. Mesylate being a good leaving group, direct displacement with sodium methanethiosulfonate does not yield the desired product. Literature methods are available for the conversion of mesylates to iodides. Having iodide as leaving group should provide a more facile route to methanesulfonate lipids than the method using bromide as a leaving group as described by Kenyon & Bruice [54].

Reaction of mesylate **10** with iodine and triphenylphosphine [62] provided a reasonable yield of the iodo-lipid but purification was hampered by triphenylphosphine and triphenylphosphine oxide formed during the reaction. However, reaction with sodium iodide (NaI) in acetone, as described by Poss & Belter [63], furnished the desired iodo-lipid **11** in excellent yield. Reaction of the iodo-lipid with sodium methanethiosulfonate (NaMTS) yielded the required methanethiosulfonate lipid **12** (Scheme 8).

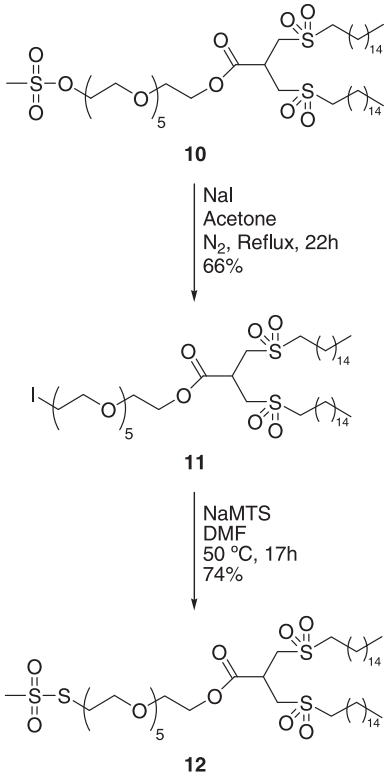

Scheme 8

Coupling reaction between PrP-React and GPIm

One volume of a concentrated solution (250 μM) of PrP-React in water was added to nine volumes of GPIm in an ethanol/water solution, resulting in a reaction mixture containing 70% ethanol in water (v/v) and a 10-fold molar excess of GPIm relative to PrP-React ([GPIm] = 250 μM; [PrP-React] = 25 μM). The solution was stirred for 2 h at room temperature and applied to a reverse-phase HPLC column (Poros R1 20, Applied Biosystems). The product, GPIm-modified protein (PrP–GPIm), was separated from unmodified protein on a water/acetonitrile gradient in the presence of 0.1% trifuoroacetic acid.

Liquid chromatography mass spectrometry (LC-MS)

All mass spectrometry was performed in the Proteomics Facility at the Institute for Animal Health as previously described [43]. Briefly, proteinaceous samples were analysed by online capillary HPLC (180 μm i.d., 5 μm bead size, 300 Å pore size, Jupiter C_{18}, Phenomenex, Macclesfield, UK). Retained components were eluted from the home-packed column by an increasing gradient of solvent B, where solvent A was 95 : 5 H_2O/acetonitrile (v/v) with 0.05% trifuoroacetic acid and solvent B was 5 : 95 H_2O/acetonitrile (v/v) with 0.05% trifuoroacetic acid. Prior to analysis, samples were diluted with solvent A to ~ 1 pmole·μL^{-1} and around 20 pmole of total protein was injected onto a homemade preconcentration trap for initial desalting. The HPLC eluate was passed directly to a Quattro II mass spectrometer (Waters UK Ltd, Elstree, UK) equipped with a continuous-flow nanospray source. The mass spectrometer was operated in positive ion mode and acquired full scan mass spectra (*m/z* 300–2100) every 5 s.

Liposome preparation

Single lipids or mixtures of lipids were mixed in chloroform solution and dried under nitrogen to form lipid films. The films were further dried overnight under vacuum to remove residual chloroform. Vesicles were prepared in 2 mM MES at pH 5 or pH 7 containing either POPC only, or a mixture of dipalmitoyl phosphatidylcholine (DPPC), cholesterol and sphingomyelin at a molar ratio of 5 : 3 : 2. Mixed DPPC/cholesterol/sphingomyelin (5 : 3 : 2) vesicles represent the composition of cholesterol- and sphingomyelin-rich domains in the plasma membrane, known as rafts, and are referred to here as raft membranes. The aqueous buffer was flushed with nitrogen prior to hydration of the lipid film. To break multilamellar vesicles, the hydrated lipid samples were subjected to five cycles of freezing and thawing (under nitrogen) using a dry ice/ethanol mixture and a 55 °C water bath. Vesicles were extruded 10 times through two 200 nm polycarbonate membranes under nitrogen at a pressure of 150 psi and a temperature of 55 °C in a stainless-steel extrusion device (Lipex Biomembranes, Vancouver, BC). The size of the liposomes was measured at 20 °C by dynamic light scattering on a DynaPro molecular sizing instrument (Hampton Research, Aliso Viejo, CA) and was found to be similar to the pore size of the membrane used for the extrusion process. The change in the size and polydispersity of the liposomes was minimal after 10 extrusion cycles [64].

Reconstitution of PrP–GPIm into liposomes

Liposomes were titrated at 20 °C with the detergent octyl-β-D-glucopyranoside (OG) (Fluka, Gillingham, UK) and light scattering at 350 nm was followed in a spectrophotometer. The midpoint of solubilization for the liposomes was determined. This concentration of OG was used in the reconstitution of PrP–GPIm into liposomes. PrP–GPIm was mixed with the appropriate amount of OG and sonicated for 15 min in a water bath at room temperature. Liposomes were added to yield final concentrations of: PrP–GPIm 10 μM, total lipid 1 mM, OG 22 mM –28 mM (depending on lipids used), in 2 mM MES buffer at pH 5 or 7. The mixture was placed in a sonicating water bath and sonicated twice at room temperature for 15 min. Samples were kept at room temperature for a further 30 min. OG was removed by extensive dialysis at room temperature against 2 mM MES buffer at pH 5 or 7.

The incorporation of PrP–GPIm into liposomes was assayed using sucrose gradient centrifugation. Discontinuous sucrose gradients were prepared, in which reconstituted PrP–GPIm in lipid vesicles was adjusted to 40% sucrose and overlaid with a 30% sucrose layer followed by a 5% sucrose layer. The samples were spun at 140 000 ***g*** in a Beckman SW50.1 rotor at 4 °C for 16 h. Eight fractions spanning the entire gradient were taken from the top and analysed by SDS/PAGE to detect protein-containing fractions. Lipid-containing fractions were identified by turbidity and dialysed against 2 mM MES at pH 5 or 7 to remove the sucrose. Liposomes were harvested by centrifugation at 140 000 ***g*** in a Beckman SW50.1 rotor at 4 °C for 1 h. The supernatant was discarded and the liposomes re-suspended in one-quarter the original volume of the reconstitution mixture in 2 mM MES at pH 5 or 7.

CD spectroscopy

CD spectra were collected at room temperature (21 °C) using a 0.1 cm path length quartz cuvette (Starna brand, Optiglass Ltd, Hainault, UK) in a Jasco J-715 spectropolarimeter (Jasco UK, Great Dunmow, UK). The bandwidth was 2 nm and the scanning speed was 200 nm·min^{-1} with a response time of 1 s and a data pitch of 0.5 nm. Typically, 16 spectra were averaged and buffer baselines were subtracted from the data.

ATR FTIR

Liposomes were deposited on a germanium internal reflection element and dried under nitrogen. Spectra were measured using a Vector 22 instrument (Bruker) fitted with a mercury cadmium telluride detector. Data are at a resolution of 4 cm^{-1} and are an average of 1024 spectra collected at room temperature (21 °C). The water vapour signal was removed from the spectra and peak fitting was performed using GRAMS AI software (ThermoGalactic, Salem, NH). Lorentzian curves were fitted to the amide I band of the PrP signal and assigned to a secondary structure type according to Byler & Susi [65].

Acknowledgements

This project has been funded by a BSEP5 grant awarded by the BBSRC to TJTP (Grant no. 88/BS516471). ACG thanks Jennifer Carswell and Dave Gerring for technical assistance and BBSRC for financial support. The manuscript was read by Professor John Ellis (Warwick University) to whom the authors are very grateful for insightful comments and suggestions.

References

1 Turk E, Teplow D, Hood L & Prusiner S (1988) Purification and properties of the cellular and scrapie hamster prion proteins. *Eur J Biochem* **176**, 21–30.
2 Oesch B, Westaway D, Walchli M, McKinley MP, Kent SB, Aebersold R, Barry RA, Tempst P, Teplow DB, Hood LE& *et al*. (1985) A cellular gene encodes scrapie PrP 27–30 protein. *Cell* **40**, 735–746.
3 Legname G, Baskakov IV, Nguyen HO, Riesner D, Cohen FE, DeArmond SJ & Prusiner SB (2004) Synthetic mammalian prions. *Science* **305**, 673–676.
4 Legname G, Nguyen HO, Baskakov IV, Cohen FE, Dearmond SJ & Prusiner SB (2005) Strain-specified characteristics of mouse synthetic prions. *Proc Natl Acad Sci USA* **102**, 2168–2173.
5 Stahl N, Borchelt DR, Hsiao K & Prusiner SB (1987) Scrapie prion protein contains a phosphatidylinositol glycolipid. *Cell* **51**, 229–240.
6 Endo T, Groth D, Prusiner SB & Kobata A (1989) Diversity of oligosaccharide structures linked to asparagines of the scrapie prion protein. *Biochemistry* **28**, 8380–8388.
7 Caughey BW, Dong A, Bhat KS, Ernst D, Hayes SF & Caughey WS (1991) Secondary structure analysis of the scrapie-associated protein PrP 27–30 in water by infrared spectroscopy. *Biochemistry* **30**, 7672–7680.
8 Pan KM, Baldwin M, Nguyen J, Gasset M, Serban A, Groth D, Mehlhorn I, Huang Z, Fletterick RJ, Cohen FE *et al*. (1993) Conversion of alpha-helices into beta-sheets features in the formation of the scrapie prion proteins. *Proc Natl Acad Sci USA* **90**, 10962–10966.
9 Haire LF, Whyte SM, Vasisht N, Gill AC, Verma C, Dodson EJ, Dodson GG & Bayley PM (2004) The crystal structure of the globular domain of sheep prion protein. *J Mol Biol* **336**, 1175–1183.
10 Wuthrich K & Riek R (2001) Three-dimensional structures of prion proteins. *Adv Protein Chem* **57**, 55–82.
11 Hornshaw MP, McDermott JR, Candy JM & Lakey JH (1995) Copper binding to the N-terminal tandem repeat region of mammalian and avian prion protein: structural studies using synthetic peptides. *Biochem Biophys Res Commun* **214**, 993–999.
12 Brown DR, Qin K, Herms JW, Madlung A, Manson J, Strome R, Fraser PE, Kruck T, von Bohlen A, Schulz-Schaeffer W *et al*. (1997) The cellular prion protein binds copper *in vivo*. *Nature* **390**, 684–687.
13 Viles JH, Cohen FE, Prusiner SB, Goodin DB, Wright PE & Dyson HJ (1999) Copper binding to the prion protein: structural implications of four identical cooperative binding sites. *Proc Natl Acad Sci USA* **96**, 2042–2047.
14 Burns CS, Aronoff-Spencer E, Legname G, Prusiner SB, Antholine WE, Gerfen GJ, Peisach J & Millhauser GL (2003) Copper coordination in the full-length, recombinant prion protein. *Biochemistry* **42**, 6794–6803.
15 Hornemann S, Schorn C & Wuthrich K (2004) NMR structure of the bovine prion protein isolated from healthy calf brains. *EMBO Rep* **5**, 1159–1164.
16 Govaerts C, Wille H, Prusiner SB & Cohen FE (2004) Evidence for assembly of prions with left-handed beta-helices into trimers. *Proc Natl Acad Sci USA* **101**, 8342–8347.
17 Wille H, Michelitsch MD, Guenebaut V, Supattapone S, Serban A, Cohen FE, Agard DA & Prusiner SB (2002) Structural studies of the scrapie prion protein by electron crystallography. *Proc Natl Acad Sci USA* **99**, 3563–3568.
18 Shyng SL, Huber MT & Harris DA (1993) A prion protein cycles between the cell surface and an endocytic compartment in cultured neuroblastoma cells. *J Biol Chem* **268**, 15922–15928.
19 Naslavsky N, Stein R, Yanai A, Friedlander G & Taraboulos A (1997) Characterization of detergent-insoluble complexes containing the cellular prion protein and its scrapie isoform. *J Biol Chem* **272**, 6324–6331.
20 Sunyach C, Jen A, Deng J, Fitzgerald KT, Frobert Y, Grassi J, McCaffrey MW & Morris R (2003) The mechanism of internalization of glycosylphosphatidylinositol-anchored prion protein. *EMBO J* **22**, 3591–3601.
21 Caughey B, Race RE, Ernst D, Buchmeier MJ & Chesebro B (1989) Prion protein biosynthesis in scrapie-infected and uninfected neuroblastoma cells. *J Virol* **63**, 175–181.

22 Caughey B, Raymond GJ, Ernst D & Race RE (1991) N-Terminal truncation of the scrapie-associated form of PrP by lysosomal protease(s): implications regarding the site of conversion of PrP to the protease-resistant state. *J Virol* **65**, 6597–6603.
23 Kaneko K, Vey M, Scott M, Pilkuhn S, Cohen FE & Prusiner SB (1997) COOH-Terminal sequence of the cellular prion protein directs subcellular trafficking and controls conversion into the scrapie isoform. *Proc Natl Acad Sci USA* **94**, 2333–2338.
24 Harris DA (1999) Cellular biology of prion diseases. *Clin Microbiol Rev* **12**, 429–444.
25 Naslavsky N, Shmeeda H, Friedlander G, Yanai A, Futerman AH, Barenholz Y & Taraboulos A (1999) Sphingolipid depletion increases formation of the scrapie prion protein in neuroblastoma cells infected with prions. *J Biol Chem* **274**, 20763–20771.
26 Prusiner SB, Scott MR, DeArmond SJ & Cohen FE (1998) Prion protein biology. *Cell* **93**, 337–348.
27 Taraboulos A, Scott M, Semenov A, Avrahami D, Laszlo L, Prusiner S & Avraham D (1995) Cholesterol depletion and modification of COOH-terminal targeting sequence of the prion protein inhibit formation of the scrapie isoform. *J Cell Biol* **129**, 121–132. [Published erratum (1995) *J Cell Biol* **130**, 501.]
28 Vey M, Pilkuhn S, Wille H, Nixon R, DeArmond SJ, Smart EJ, Anderson RGW, Taraboulos A & Prusiner SB (1996) Subcellular colocalization of the cellular and scrapie prion proteins in caveolae-like membranous domains. *Proc Natl Acad Sci USA* **93**, 14945–14949.
29 Borchelt D, Taraboulos A & Prusiner S (1992) Evidence for synthesis of scrapie prion proteins in the endocytic pathway. *J Biol Chem* **267**, 16188–16199.
30 Caughey B & Raymond G (1991) The scrapie-associated form of PrP is made from a cell surface precursor that is both protease- and phospholipase-sensitive. *J Biol Chem* **266**, 18217–18223.
31 Jeffrey M, McGovern G, Goodsir CM, Brown KL & Bruce ME (2000) Sites of prion protein accumulation in scrapie-infected mouse spleen revealed by immuno-electron microscopy. *J Pathol* **191**, 323–332.
32 Critchley P, Kazlauskaite J, Eason R & Pinheiro TJ (2004) Binding of prion proteins to lipid membranes. *Biochem Biophys Res Commun* **313**, 559–567.
33 Kazlauskaite J, Sanghera N, Sylvester I, Venien-Bryan C & Pinheiro TJ (2003) Structural changes of the prion protein in lipid membranes leading to aggregation and fibrillization. *Biochemistry* **42**, 3295–3304.
34 Sanghera N & Pinheiro TJ (2002) Binding of prion protein to lipid membranes and implications for prion conversion. *J Mol Biol* **315**, 1241–1256.
35 Sarnataro D, Campana V, Paladino S, Stornaiuolo M, Nitsch L & Zurzolo C (2004) PrPC association with lipid rafts in the early secretory pathway stabilizes its cellular conformation. *Mol Biol Cell* **15**, 4031–4042.
36 Eberl H, Tittmann P & Glockshuber R (2004) Characterization of recombinant, membrane-attached full-length prion protein. *J Biol Chem* **279**, 25058–25065.
37 Stahl N, Baldwin MA, Hecker R, Pan KM, Burlingame AL & Prusiner SB (1992) Glycosylinositol phospholipid anchors of the scrapie and cellular prion proteins contain sialic acid. *Biochemistry* **31**, 5043–5053.
38 Mo H, Moore RC, Cohen FE, Westaway D, Prusiner SB, Wright PE & Dyson HJ (2001) Two different neurodegenerative diseases caused by proteins with similar structures. *Proc Natl Acad Sci USA* **98**, 2352–2357.
39 Nosjean O & Roux B (2003) Anchoring of glycosylphosphatidylinositol-proteins to liposomes. *Methods Enzymol* **372**, 216–232.
40 Seddon AM, Curnow P & Booth PJ (2004) Membrane proteins, lipids and detergents: not just a soap opera. *Biochim Biophys Acta* **1666**, 105–117.
41 James TL, Liu H, Ulyanov NB, Farr-Jones S, Zhang H, Donne DG, Kaneko K, Groth D, Mehlhorn I, Prusiner SB *et al.* (1997) Solution structure of a 142-residue recombinant prion protein corresponding to the infectious fragment of the scrapie isoform. *Proc Natl Acad Sci USA* **94**, 10086–10091.
42 Blanch EW, Gill AC, Rhie AG, Hope J, Hecht L, Nielsen K & Barron LD (2004) Raman optical activity demonstrates poly(1-proline) II helix in the N-terminal region of the ovine prion protein: implications for function and misfunction. *J Mol Biol* **343**, 467–476.
43 Gill AC, Ritchie MA, Hunt LG, Steane SE, Davies KG, Bocking SP, Rhie AG, Bennett AD & Hope J (2000) Post-translational hydroxylation at the N-terminus of the prion protein reveals presence of PPII structure in vivo. *EMBO J* **19**, 5324–5331.
44 Zahn R (2003) The octapeptide repeats in mammalian prion protein constitute a pH-dependent folding and aggregation site. *J Mol Biol* **334**, 477–488.
45 Riek R, Hornemann S, Wider G, Glockshuber R & Wuthrich K (1997) NMR characterization of the full-length recombinant murine prion protein, mPrP (23–231). *FEBS Lett* **413**, 282–288.
46 Zahn R, Liu A, Luhrs T, Riek R, von Schroetter C, Lopez Garcia F, Billeter M, Calzolai L, Wider G & Wuthrich K (2000) NMR solution structure of the human prion protein. *Proc Natl Acad Sci USA* **97**, 145–150.
47 Rudd PM, Wormald MR, Wing DR, Prusiner SB & Dwek RA (2001) Prion glycoprotein: structure, dynamics, and roles for the sugars. *Biochemistry* **40**, 3759–3766.
48 Safar J, Ceroni M, Gajdusek DC & Gibbs CJ Jr (1991) Differences in the membrane interaction of scrapie amyloid precursor proteins in normal and scrapie- or

Creutzfeldt-Jakob disease-infected brains. *J Infect Dis* **163**, 488–494.
49 Stahl N, Borchelt DR & Prusiner SB (1990) Differential release of cellular and scrapie prion proteins from cellular membranes by phosphatidylinositol-specific phospholipase C. *Biochemistry* **29**, 5405–5412.
50 Kazlauskaite J & Pinheiro TJ (2005) Aggregation and fibrillization of prions in lipid membranes. *Biochem Soc Symp*, 211–222.
51 Sunyach C & Checler F (2005) Combined pharmacological, mutational and cell biology approaches indicate that p53-dependent caspase 3 activation triggered by cellular prion is dependent on its endocytosis. *J Neurochem* **92**, 1399–1407.
52 Klein TR, Kirsch D, Kaufmann R & Riesner D (1998) Prion rods contain small amounts of two host sphingolipids as revealed by thin-layer chromatography and mass spectrometry. *Biol Chem* **379**, 655–666.
53 Kirby L, Birkett CR, Rudyk H, Gilbert IH & Hope J (2003) *In vitro* cell-free conversion of bacterial recombinant PrP to PrPres as a model for conversion. *J Gen Virol* **84**, 1013–1020.
54 Kenyon GL & Bruice TW (1977) Novel sulfhydryl reagents. *Methods Enzymol* **47**, 407–430.
55 Ferris A (1955) The action of mineral acid on diethyl bis(hydroxymethy) malonate. *J Org Chem* **20**, 780–787.
56 Ansari AA, Frejd T & Magnusson G (1987) 3-Bromo-2-bromomethylpropyl glycosides in the preparation of double-chain bis-sulfide neo-glycolipids. *Carbohydr Res* **161**, 225–233.
57 Zhang ZY & Magnusson G (1994) Synthesis of double-chain bis-sulfone neoglycolipids of the 2″-deoxyglobotriose, 3″-deoxyglobotriose, 4″-deoxyglobotriose, and 6″-deoxyglobotriose. *Carbohydr Res* **262**, 79–101.
58 Georges C, Lewis TJ, Llewellyn JP, Salvagno S, Taylor DM, Stirling CJM & Vogel V (1988) Chiral sulfur-containing molecules in Langmuir-Blodgett films. *J Chem Soc Faraday Trans* **I**, 1531–1542.
59 Bertozzi CR & Bednarski MD (1991) The synthesis of heterobifunctional linkers for the conjugation of ligands to molecular probes. *J Org Chem* **56**, 4326–4329.
60 Whitesell JK & Reynolds D (1983) Resolution of chiral alcohols with mandelic-acid. *J Org Chem* **48**, 3548–3551.
61 King SA, Pipik B, Thompson AS, Decamp A & Verhoeven TR (1995) Efficient synthesis of carbapenems via the oxalimide cyclization – manipulation of protecting groups at the oxalimide stage. *Tetrahedron Lett* **36**, 4563–4566.
62 Kocienski PJ, Pelotier B, Pons JM & Prideaux H (1998) Asymmetric syntheses of panclicins A-E via [2 + 2] cycloaddition of alkyl (trimethylsilyl) ketenes to a beta-silyloxyaldehyde. *J Chem Soc Perkin Trans* **1**, 1373–1382.
63 Poss AJ & Belter RK (1987) Diethyl 3-iodopropynephosphonate – an alkylative beta-keto phosphonate equivalent. *J Org Chem* **52**, 4810–4812.
64 Mui B, Chow L & Hope MJ (2003) Extrusion technique to generate liposomes of defined size. *Methods Enzymol* **367**, 3–14.
65 Byler DM & Susi H (1986) Examination of the secondary structure of proteins by deconvolved FTIR spectra. *Biopolymers* **25**, 469–487.